International Journal of Rock Mechanics & Mining Sciences 71 (2014) 1–11

Contents lists available at ScienceDirect

International Journal of Rock Mechanics & Mining Sciences

journal homepage: www.elsevier.com/locate/ijrmms

Non-associative limit analysis of the toppling-sliding failure of rock slopes

Ahmed Faysal A. Babiker [a], Colin C. Smith [a,*], Matthew Gilbert [a], John P. Ashby [b]

[a] Department of Civil & Structural Engineering, University of Sheffield, Mappin Street, Sheffield S1 3JD, UK
[b] Ashby Consultants Limited, 1/26 Bassett Road, Auckland 1050, New Zealand

ARTICLE INFO

Article history:
Received 23 February 2013
Received in revised form
4 March 2014
Accepted 22 June 2014

Keywords:
Rock slope stability
Toppling-sliding
Non-associative friction
Plasticity
Limit analysis

ABSTRACT

Limit analysis is a powerful procedure which is widely used in geotechnical engineering for the analysis of collapse states. However, when applied to toppling-sliding failures in rock slopes, overestimates of stability can arise, and hence limit equilibrium and DEM approaches have proved more popular. In this paper it is shown that limit analysis tends to overestimate stability due to the presence of potentially unrealistic dilatancy at the joints. To address this, a modified plastic limit analysis procedure incorporating a non-associative, low dilation, friction model is proposed. Originally developed to assess the stability of masonry walls, the procedure is here extended to allow an envelope of potential solutions to be obtained. The numerical results obtained are found to closely match both analytical and experimental results from the literature, demonstrating the significant promise of the procedure.

1. Introduction

1.1. Background

The influence of geological discontinuities on the stability of rock slopes and in particular on their modes of failure had been recognised by a number of workers by the 1960s, as documented in the literature, e.g. Hoek and Bray [1]. Examples of rock slope failure modes are shown in Fig. 1, and include planar 2-dimensional wedge, 3-dimensional wedge and circular failure modes. Plane failures occur by sliding on a single discontinuity, whereas wedge failures require two or more intersecting discontinuities. Although circular arc failures were originally recognised in soil slopes, they can occur in large scale rock slopes where the discontinuities are closely spaced, or where the intervening rock is sufficiently weak to fail internally.

Toppling failure involves rotation of jointed columns about pivot points. Pure toppling failure only occurs in very steep or overhanging slopes. On the other hand, toppling-sliding failure can occur in flatter slopes or in larger scale slopes, where toppling columns force the rock near the toe of the slope to fail by sliding or shearing through intact material. The resulting failure surface is often approximately circular in shape. Studies of toppling-sliding failure were initiated in the late 1960s and early 1970s using physical models, e.g. Ashby [2]. Subsequently various workers have identified the toppling-sliding mechanism in failures observed in the field [3].

1.2. Toppling-sliding stability analysis

Various numerical and analytical procedures have been proposed to solve problems involving toppling-sliding failure of rock slopes. Considering numerical procedures first, the distinct element method (DEM) originally developed by Cundall [4] has been applied by workers such as Ashby [2], Ishida et al. [5] and Lanaro et al. [6]. With DEM large displacements and separation of blocks can be modelled by incrementally solving equations of motion, using an explicit finite-difference method that requires small time steps. Corners of blocks are rounded to model crushing, thereby eliminating singularities. In order to balance the kinetic energy in the system a damping coefficient is introduced, tailored according to block size.

Considering analytical procedures, analysis of rock slope stability is usually undertaken by a combination of kinematic analysis and limit equilibrium analysis. Kinematic analysis involves interpreting the geometry of the geological discontinuities and the slope to determine whether failure by a given mechanism is feasible. The rock slope stability analysis is then carried out using a limit equilibrium analysis of the given geometry as shown by e.g. Goodman and Bray [7] and Hoek and Bray [1]. However in a limit equilibrium analysis the goal is to ensure global equilibrium is satisfied, regardless of kinematic considerations, i.e. the failure mechanism identified need not actually be kinematically admissible. Since then, in the absence of other readily available tools,

* Corresponding author. Tel.: +44 114 2225717.
E-mail address: c.c.smith@sheffield.ac.uk (C.C. Smith).

http://dx.doi.org/10.1016/j.ijrmms.2014.06.008

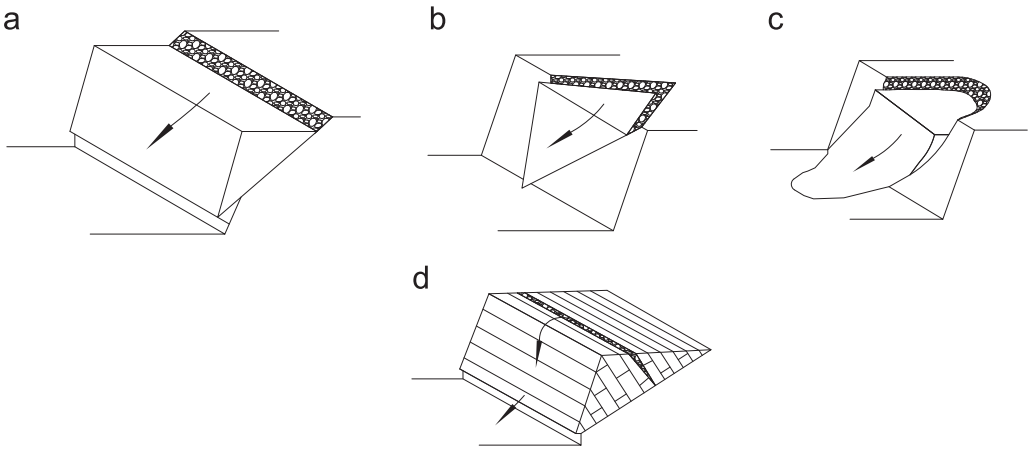

Fig. 1. Modes of failure in rock slopes (after Hoek and Bray [1]). (a) *Plane*, (b) *wedge*, (c) *circular* and (d) *toppling -sliding*.

limit equilibrium procedures have been favoured by most workers in the field, e.g. Wyllie [8], Zanbak [9], Aydan and Kawamoto [10], Adhikary et al. [11], and Sagaseta et al. [12].

In recent years, research on rock slope stability has continued. Many researchers have continued to focus on toppling-sliding failures, e.g. Liu et al. [13], Tatone and Grasselli [14], and Liu et al. [15], with limit equilibrium methods generally used to obtain solutions. Additionally, some researchers have considered 'flexural toppling' scenarios, in which flexural cracking of blocks is considered (e.g., [16–18]) or 'block-flexure' toppling, in which overturning of some blocks is accompanied by flexural cracking of others (e.g. [19]). In this paper, the focus will be on modelling toppling-sliding failures, without flexural cracking, though now utilising a numerical approach based on the principles of limit analysis rather than limit equilibrium, which has been the predominant methodology used in this field to date.

1.3. Limit analysis

In limit analysis (see e.g. [20]) both global equilibrium and kinematic admissibility are enforced, potentially leading to more rigorous solutions when compared to limit equilibrium methods which generally consider equilibrium only and often require additional assumptions about forces acting in the system. The only issue is that in conventional limit analysis the relationship between inter-block forces and displacements is governed by the associative flow rule, which means that sliding along a joint will be accompanied by separation, or 'dilatancy' [21]. Thus a tangential displacement δ_t along a joint will be accompanied by a normal displacement δ_n, according to the following equation:

$$\delta_n = \delta_t \tan \psi, \tag{1}$$

where ψ is the angle of dilatancy. This will equal the angle of friction ϕ when using a conventional limit analysis approach due to the normality principle, leading to what is termed 'associative friction'. This theoretical principle makes the analysis of the problem relatively straightforward by eliminating a source of static indeterminacy and allows the application of the powerful upper and lower bound theorems of plasticity. However, little or no dilation is typically observed in practice (i.e. Fig. 2b vs. 2a). While this does not tend to affect analysis of sliding failures due to the simple mechanics and kinematics involved, analysis of toppling-sliding failure is complicated by the indeterminacy that affects the location of the points of contact between blocks and the forces at those points. This can lead to a conventional limit analysis overestimating the actual stability of rock slopes, given that these generally comprise tightly packed assemblages of blocks.

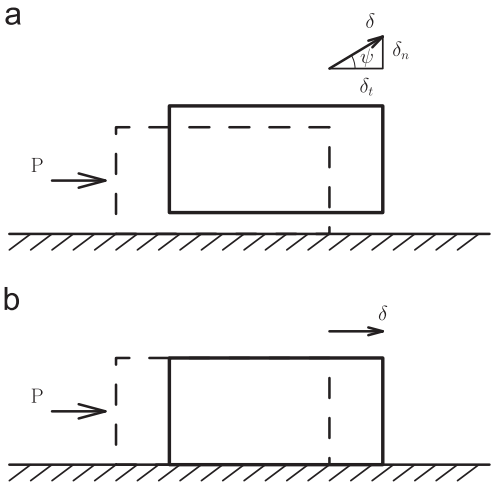

Fig. 2. Sliding along a joint: (a) with dilation ('associative friction' when $\psi=\phi$), (b) no dilation ('non-associative friction', unless $\phi=0$).

However, since the essential features of a limit analysis approach are otherwise attractive, here a method of modelling problems with a reduced, more realistic, level of dilation within a limit analysis framework is explored, leading to a novel non-associative friction (i.e. $\psi \neq \phi$) analysis.

1.4. Aims

The aims of this paper are to:

(i) Provide details of a general purpose method that can generate kinematically viable non-associative collapse mechanisms for sliding, toppling, or combined toppling-sliding, failures.
(ii) Establish the range of non-associative collapse loads relevant to a particular collapse mechanism.
(iii) Validate the proposed methodology using theoretical and experimental results available in the literature.

An algorithm previously applied to assemblages of masonry blocks [22] will be used to address (i), while a new numerical procedure will be presented to address (ii). Given the strongly non-associative character of toppling-sliding rock slope failures, examples of experimental data were chosen from the rock mechanics literature to address (iii).

2. Analysis of simple systems

2.1. Single block failure

For single blocks of the sort shown in Fig. 3, the conditions for failure can involve sliding or toppling, and limit equilibrium and limit analysis approaches will be identical. Sliding occurs when the tangential component of the weight ($W \sin \alpha$) is greater than the shear resistance at the base ($\mu W \cos \alpha$), where W is the weight of the block, α is the dip angle and $\mu = \tan \phi$ is the friction coefficient. Sliding will thus occur when $\alpha > \phi$. Toppling, on the other hand, involves a column rotating about a pivot point or 'hinge', taken to be at the lowest corner point if the block is assumed to be rigid, represented by point O in Fig. 3. Stability requires that the weight W acts through a point on the line of contact between the base and the block. The large block in Fig. 3 could thus fail by toppling, while both blocks may fail by sliding if $\alpha > \phi$.

Stability may also be assessed in a more general way by perturbing the system by some means to initiate collapse. Physical experiments are typically performed using a tilting table. In this approach failure is identified by the tilt angle (α) at which collapse occurs. As the tilt angle of the base is increased, the horizontal components of the weight driving sliding or rotation increase. This is analogous to applying an increasing horizontal body force, achieved in practice by applying a horizontal force equal in magnitude to the self weight of each block multiplied by a load factor, λ. The tilt angle can then be obtained from the following relation:

$$\tan \alpha = \frac{\lambda W}{W} \tag{2}$$

And hence:

$$\alpha = \tan^{-1} \lambda \tag{3}$$

It should be noted that in the equivalent tilted analysis, gravity has also increased by a factor of $\sqrt{1+\lambda^2}$. However, this does not affect the limiting tilt angle for a purely frictional problem.

2.2. Effect of associativity on the solution

For a single block, the flow rule has no effect on the solution (i.e. the amount of dilatancy which occurs does not affect the answer). Therefore a standard limit analysis is sufficient to assess stability. However, in general, a problem will not be composed of a single block or column but an assemblage of blocks that may slide and/or topple, and will in general interact with each other in a statically indeterminate way. It is possible to analyse such problems using limit analysis, but this is likely to provide a non-conservative estimate of stability when the number of blocks increases. It is therefore necessary to take the kinematics of the problem into consideration and in particular the effects of non-associativity.

As mentioned earlier, imposing an associative flow rule results in restrictive mechanisms that may result in non-conservative collapse loads. Non-associative friction removes these kinematic restrictions by allowing sliding with reduced dilation. This leads to equilibrium systems with greater degrees of freedom due to fewer joints between blocks undergoing relative movement (and thus being constrained to be at yield). This can be illustrated by examining a simple two-block system, presented in the next section.

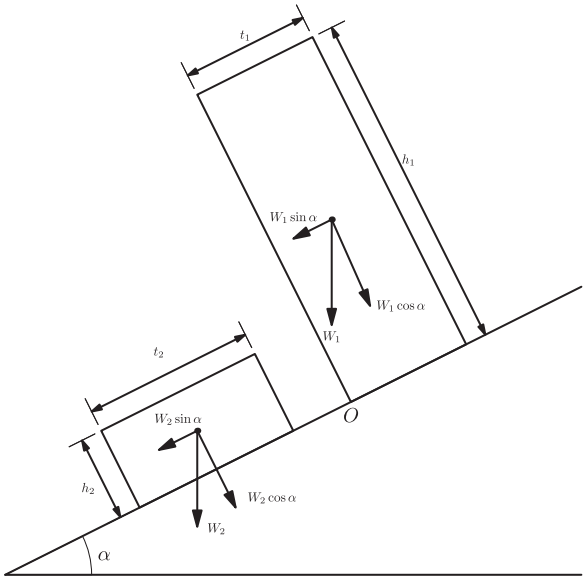

Fig. 3. Sliding and toppling: forces acting on a single block.

2.3. Two-block failure: sliding and toppling

For the two-block system shown in Fig. 4, toppling failure can occur when the larger of the two blocks rotates while the smaller block slides. In this problem it will be shown that the frictional resistance at the point of contact (X) between the two blocks governs the range and value of the load factor λ. For the associative case, shown in Fig. 4a, the shear force acting on the large block at X is mobilised in the vertically upwards direction due to kinematic considerations. However, for the non-associative case shown in Fig. 4b, since there is no relative movement (assuming

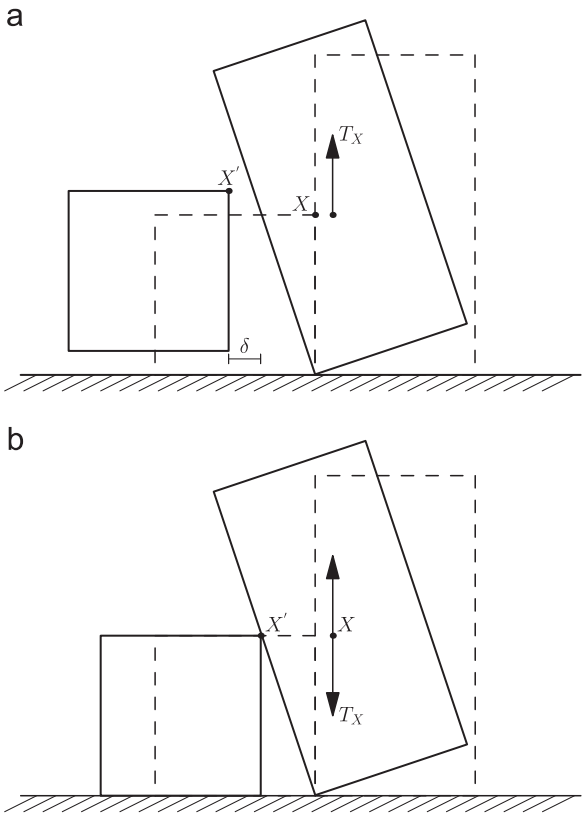

Fig. 4. Two-block failure: the influence of dilation (δ) on stability (assuming small displacement theory holds). (a) Associative mechanism: shear force at X in the positive vertical direction and (b) non-associative mechanism: shear force at X may act upwards or downwards.

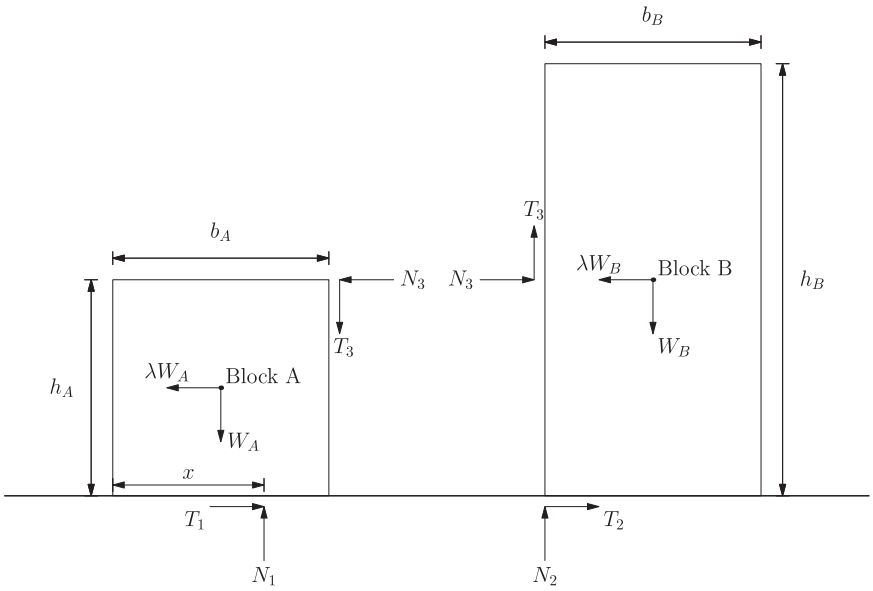

Fig. 5. Two-block failure: free body diagrams.

Table 1
Two block failure: block equilibrium conditions.

Condition	Block A	Block B
Horizontal	$T_1=\lambda W_A+N_3$	$N_3+T_2=\lambda W_B$
Vertical	$N_1=W_A+T_3$	$N_2+T_3=W_B$
Moment	$\frac{T_1h_A}{2}+\frac{N_3h_A}{2}+N_1\left(x-\frac{b_A}{2}\right)=\frac{T_3b_A}{2}$ $\therefore\ x=\frac{(T_3+N_1)b_A-(T_1+N_3)h_A}{2N_1}$	$\frac{T_2h_B}{2}=N_2\left(\frac{b_B}{2}\right)+T_3\left(\frac{b_B}{2}\right)$ $\therefore\ T_2h_B=W_Bb_B$

Table 2
Two block failure: joint sliding yield conditions.

Condition	Joint 1	Joint 2	Joint 3
Sliding	$T_1=N_1\ \tan\ \phi$	$T_2\le N_2\tan\ \phi$	$-N_3\tan\phi\le T_3\le N_3\ \tan\ \phi$

instantaneous displacements and zero dilation), the force magnitude and direction will be bracketed but not specifically defined.

2.3.1. Analysis of a sliding and toppling two-block system

Fig. 5 shows the free body diagram for the two-block system considered in Fig. 4. By considering the equilibrium and yield of the two blocks, associative and non-associative solutions for the sliding of Block A and toppling of Block B can be derived.

If the unit weight of the blocks is γ, then the weight W of each block is given as follows:

$$W_A=\gamma h_Ab_A \tag{4}$$

$$W_B=\gamma h_Bb_B \tag{5}$$

Failure is induced by the application of a horizontal body force λW to each block, where λ provides a measure of the tilt required to initiate collapse, see Eq. (3). The equilibrium and yield conditions for the two blocks are shown in Tables 1 and 2. Joint 3, between Block A and Block B, will mobilise a strength m, such that

$$T_3=mN_3\ \tan\ \phi \tag{6}$$

where $-1\le m\le 1$.

It is also necessary to ensure that the normal force N_1 acts within the width of the base of Block A, i.e:

$$0\le x\le b_A \tag{7}$$

In order to formulate the problem λ must be defined as a function of T_1,N_1,T_2,N_2,T_3,N_3. Substituting the vertical equilibrium equation for Block A and sliding yield equation for Joint 1 into the horizontal equilibrium equation for Block A and rearranging gives

$$N_3=(W_A+T_3)\tan\ \phi-\lambda W_A \tag{8}$$

Substituting the horizontal and moment equilibrium equations of Block B into Eq. (8) and rearranging gives

$$T_3=\frac{1}{\tan\ \phi}\left(\lambda(W_A+W_B)-\frac{W_Bb_B}{h_B}\right)-W_A \tag{9}$$

The mobilised strength $m=T_3/(N_3\ \tan\phi)$ on the joint between the blocks can be determined for various values of λ. For each solution it must be checked that $T_2\le\ N_2\ \tan\ \phi$ and $0<x<b_A$ are satisfied. The minimum non-associative solution is found when $m=-1$ whilst the maximum is found when $m=1$.

The influence of the angle of friction on the associative load and the minimum non-associative load is shown in Fig. 6 for the case of a 1×1 (height $\times$ width) Block A and a 2×1 Block B.

For $\phi=36^\circ$ the associative solution can be shown to be $\lambda=0.6165$, while the minimum non-associative solution can be shown to be $\lambda=0.5559$, a difference of 9%, with possible non-associative solutions λ_{NA} bracketed as follows: $0.5559\le\ \lambda_{NA}\le 0.6165$. It will be shown later that the difference between the non-associative and associative results will in general increase as the number of blocks increases. It is therefore important to model non-associative friction for these types of problem.

3. Identification of non-associative collapse mechanisms

Basic limit analysis formulations for problems involving assemblages of rigid blocks with associative frictional joints have been considered by workers such as Livesley [23] and Gilbert and Melbourne [24]. In the current approach the problem considered involves an assemblage of rigid blocks separated by joints which cannot resist tensile forces. Each block may rock and/or slide relative to an adjacent block. Each block has three degrees of

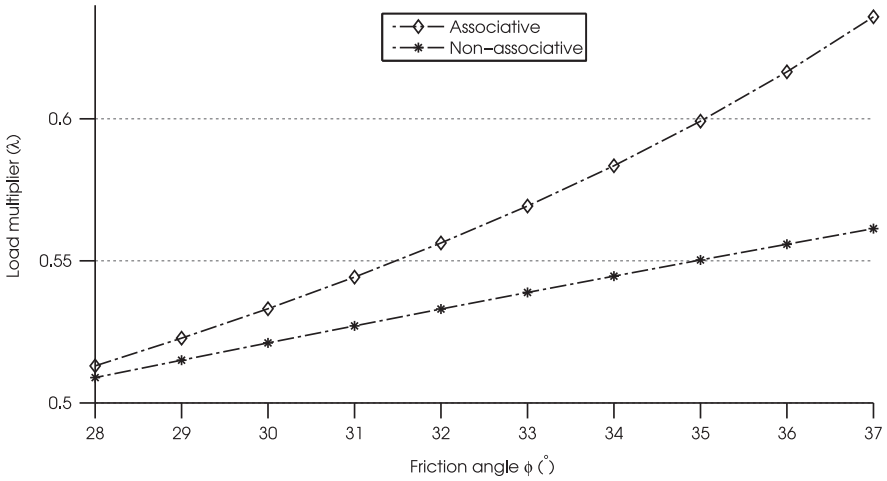

Fig. 6. The influence of friction angle (ϕ) on the associative and minimum non-associative load factor λ for the two block problem.

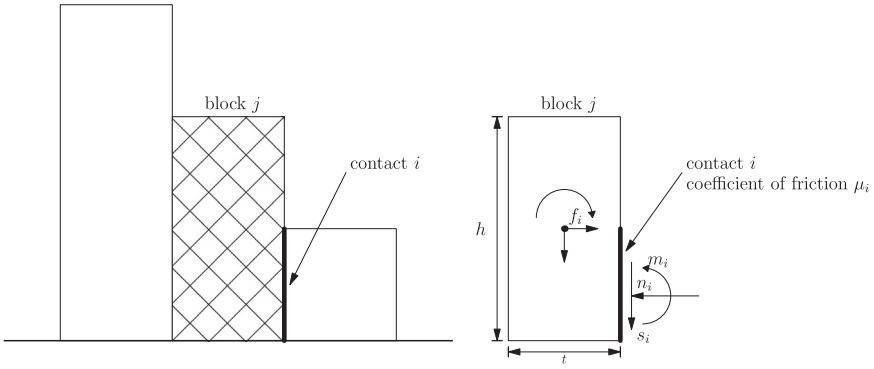

Fig. 7. Block j geometry and properties, and contact forces for joint i.

freedom around its centroid: horizontal displacement, vertical displacement and rotation. Correspondingly three forces act along the joints between blocks: shear force, normal force and moment, as shown in Fig. 7. Yield conditions govern the failure criterion along each joint i between blocks for both slip and rotation. Fig. 8a and b shows a typical failure surfaces for toppling and sliding at any contact i. It can be seen that both criteria depend on the normal force which is the unknown parameter in these type of problems. When a classical equilibrium formulation is employed, this involves maximising a load factor while ensuring that each block is in equilibrium and that yield is not violated at any joint. Considering an assemblage of b blocks and c joints, this problem can be formulated as a linear programming (LP) problem as follows:

$max\ \lambda$

subject to

$$\mathbf{Bq}-\lambda\mathbf{f}_L=\mathbf{f}_D \tag{10}$$

$$\left.\begin{array}{l} m_i \le 0.5 n_i h_i \\ m_i \ge -0.5 n_i h_i \\ s_i \le \mu_i n_i \\ s_i \ge -\mu_i n_i \end{array}\right\} \quad \text{for each joint between blocks } i=1,\ldots,c \tag{11}$$

where λ is the load factor, $\mathbf{B}$ is a suitable $(3b \times 3c)$ equilibrium matrix, enforcing horizontal, vertical and moment equilibrium, and $\mathbf{q}$ and $\mathbf{f}$ are respectively vectors of joint forces and block loads. Thus $\mathbf{q}^{\mathbf{T}}=\{n_1,s_1,m_1,n_2,s_2,m_2..n_c,s_c,m_c\}$; $\mathbf{f}=\mathbf{f}_D+\lambda\mathbf{f}_L$ where $\mathbf{f}_D$ and $\mathbf{f}_L$ are respectively vectors of dead and live loads. Joint and block forces, dimensions and frictional properties are shown in Fig. 7. Using this formulation the LP variables are the contact forces for any joint i, i.e: n_i, s_i, m_i (where $n_i \ge 0$; s_i, m_i are free variables). Eq. (11) enforces joint yield conditions for each joint in the n-s-m domain and defines the failure criteria governed both by sliding and toppling. Note that although the associative flow rule is not *explicitly* referred to in this formulation, it is *implicitly* enforced (e.g. see [23]).

More recently, extended formulations which allow non-associative frictional joints to be treated have been proposed by workers such as Ferris and Tin-Loi [25], Orduña and Lourenco [26] and Gilbert et al. [22]. Here the latter approach is used as a starting point.

3.1. Limit analysis formulation for discrete block rotation and sliding (after Gilbert et al. [22])

In essence the approach proposed by [22] involves the successive solution of simple associative problems. Thus, referring to Fig. 9a, consider a point A representing the forces acting on a joint between blocks and lying on the Mohr–Coulomb failure surface (indicated by the solid line), where the normal and shear forces are N and T respectively. The associated flow rule clearly requires $\psi=\phi$ (i.e. flow in the direction of the solid arrow), whereas the required non-associated flow, with $\psi=0$, will be in the direction indicated by the dashed arrow. In order to ensure $\psi=0$, while still utilising an associative analysis, a fictitious failure surface can be constructed by rotating the yield surface about the force point

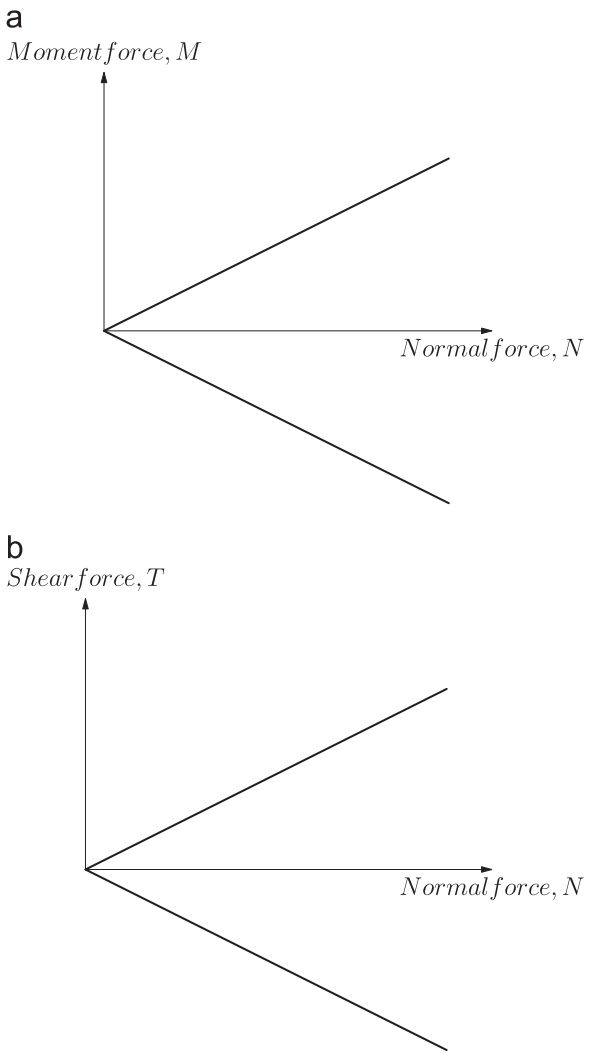

Fig. 8. Yield domains. (a) Toppling and (b) sliding.

obtained for the associative solution, represented by the dashed line ($\hat{C} = N \tan \phi$). This still correctly limits the shear force at A provided the normal force remains constant. In principle the failure surfaces corresponding to all joint forces would be replaced in this way and the problem solved again. However there is no guarantee that the normal forces will remain constant after re-solving, and hence a number of iterations may be required before a converged solution is reached, as shown in Fig. 9b. Assuming a converged solution can be obtained, this solution will satisfy both the original failure surface at all points, and will ensure that flow is non-associative as required (the flow vector is also normal to the fictitious yield surface). This will be a valid non-associative solution, though is not necessarily unique.

Extending the process to all joints between blocks in the problem allows a numerical solution procedure to be developed as follows:

1. Solve the problem initially assuming associative flow. The initial normal $N_{i,0}$ and shear $T_{i,0}$ forces can be extracted from the solution for each joint i, together with the collapse load factor λ_0.
2. At the next iteration k the modified shear strength parameter $\hat{C}_{i,k}$ for joint i can be computed using the normal force from the previous iteration $N_{i,k-1}$ as follows:

$$\hat{C}_{i,k} = N_{i,k-1} \tan \phi \tag{12}$$

where ϕ is the actual material angle of friction.

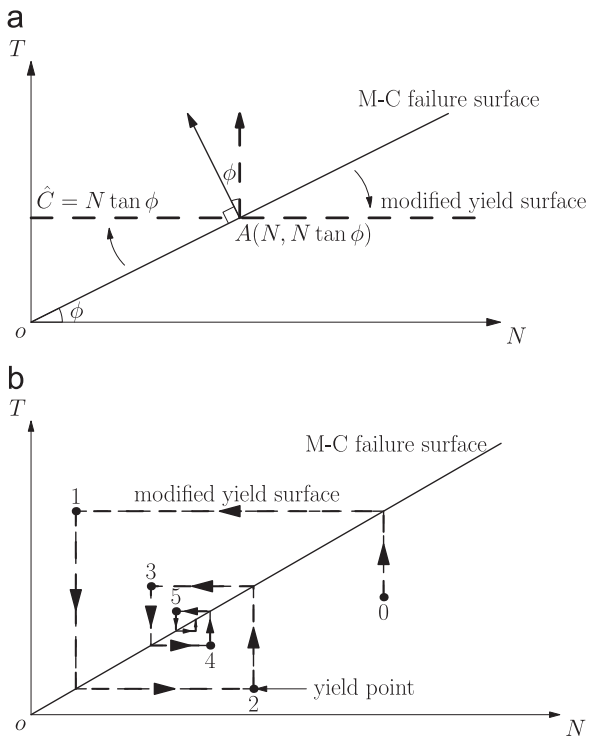

Fig. 9. Non-associative algorithm: original and modified failure surfaces. (a) Constant normal force at joint for a single iteration and (b) variable normal force at joint for multiple iterations.

3. Solve the associative problem using parameters $\hat{C}_{i,k}$ to obtain new values of $N_{i,k}$, $T_{i,k}$, and λ_k.
4. If $k > 1$ and $|\lambda_k - \lambda_{k-1}|/\lambda_k < \epsilon$, where ϵ is the specified solution tolerance, and violation of the real failure surface is not detected at any discontinuity i, then the algorithm stops.
5. If there is no convergence the process is repeated from step (ii) until convergence is reached.

This algorithm was implemented using a modified version of a C++ code described by [22] which utilised the Mosek LP solver [27].

As in most limit analysis procedures, it is possible to model horizontal body forces. This is achieved by applying a factored block weight (λW) horizontally in order to cause failure. Also, for the sake of simplicity a cohesionless material interface with dilation angle ψ taken as zero will be considered in this paper, though the same basic method can potentially be applied to problems with a non-zero angle of dilation.

4. Min–max procedure to bracket the range of possible solutions

The algorithm presented in the previous section is capable of generating kinematically valid collapse mechanisms. However, as was demonstrated in the example considered in Section 2.3, the value of the collapse load factor will generally be non-unique, since most problems encountered will be statically indeterminate. It is therefore of interest to establish the likely range of possible load factors which can be applied.

Considering the mechanism identified as being critical, the force distribution along yielding joints can be fixed and defined by the yield criterion (i.e. $T = N \tan \phi$ when sliding failure is involved). On the other hand, to allow a range of possible solutions to be identified, forces along non-yielding joints can be left free to

take different values subject to equilibrium being enforced, and yield not being violated. Thus the following procedure is proposed:

(i) Obtain a *non-associative* solution using the procedure described in Section 3.
(ii) Setup a new *associative* analysis, but this time prescribing that yield must occur along all joints that yielded in the mechanism identified in (i).
(iii) Solve the problem searching for the minimum load factor, λ_{min}.
(iv) Solve the problem searching for the maximum load factor, λ_{max}.

It should be noted that the initial non-associative solution referred to in (i) and the maximised solution found in (iv) will both correspond to kinematically compatible collapse mechanisms. (N. B. although an equilibrium formulation has been used, collapse mechanisms can be identified using LP duality principles, e.g. see Charnes et al. [28].) However, the minimised solution from (iii) will not in general correspond to a mechanism that is kinematically viable, since the solution derives from a minimisation process. However in this case the original mechanism should be compatible with the solution found and thus remains valid.

The procedure described has been tested and found to be robust as long as a viable mechanism is identified in step (i) of the procedure. However it may sometimes be found to be difficult to precisely define the form and extent of a mechanism, and whether yielding is truly occurring in a given joint. This is particularly the case for problems involving numerous blocks, with very small relative movements between some blocks. After investigating the issue further it was found that relative displacement was actually the most reliable indicator of yielding, and a constant threshold value of 10^{-5} was chosen for use in the examples described in this paper.

5. Case studies

5.1. Example 1: Goodman and Bray (analytical)

The following is a limit equilibrium block-toppling problem based on an example proposed by Goodman and Bray [7], published by Hoek and Bray [1] and reprinted by Wyllie and Mah [29]. The objective is to calculate the factor of safety and required bolting force to prevent toppling failure for the problem illustrated in Fig. 10.

A rock face 92.5 m high is cut at an angle of 56.6° in a layered rock mass dipping at 60° into the face. The width of each block is 10 m and the angle of the slope above the crest of the cut is 4°, the base of each block is stepped by 1 m. Based on this geometry, there are 16 blocks formed between the toe and crest of the slope. The friction angles on the faces and bases of the blocks are 38.15° and the unit weight of the rock is 25 kN/m^3.

The limit equilibrium analysis proceeds by evaluating the stability of each block, starting from block 16 until the toe block (1) is reached. According to the analytical results the top three blocks (16, 15, 14) and the three toe blocks (3, 2, 1) slide, while the rest of the blocks fail by toppling. The analytical calculations are made possible by assuming the supporting slope is stepped, thereby eliminating indeterminacy of the contact point locations between adjacent toppling blocks. The result of the analysis performed indicates that the system is unstable, and that the angle of friction would have to be increased to 39° to make it stable.

The same problem was modelled using the proposed approach. In order to compare the analytical results with the proposed approach, the angle of friction was increased until a tilt angle of 30° was obtained (this is equal to the tilt angle pre-assumed in the analytical solution). The angle of friction required to achieve this was found to be approximately 39.1°. The failure mechanism obtained was virtually identical to that identified by Goodman & Bray, though with block 3 (hatched in Fig. 10) now predicted to fail by toppling rather than sliding.

A further analysis was carried out by extracting and comparing the shear and normal forces acting on the base and sides of each block; the results are shown in Fig. 11. It can be seen that the there is a difference in the forces acting on the toe blocks due to the difference in mechanism mentioned above. For blocks in the toppling and stable zones (i.e. blocks 4–16), the forces are approximately the same.

In summary, the results from this example demonstrate that the proposed non-associative procedure is capable of approximately reproducing results from the widely used limit equilibrium procedure developed by Goodman and Bray [7]. However a

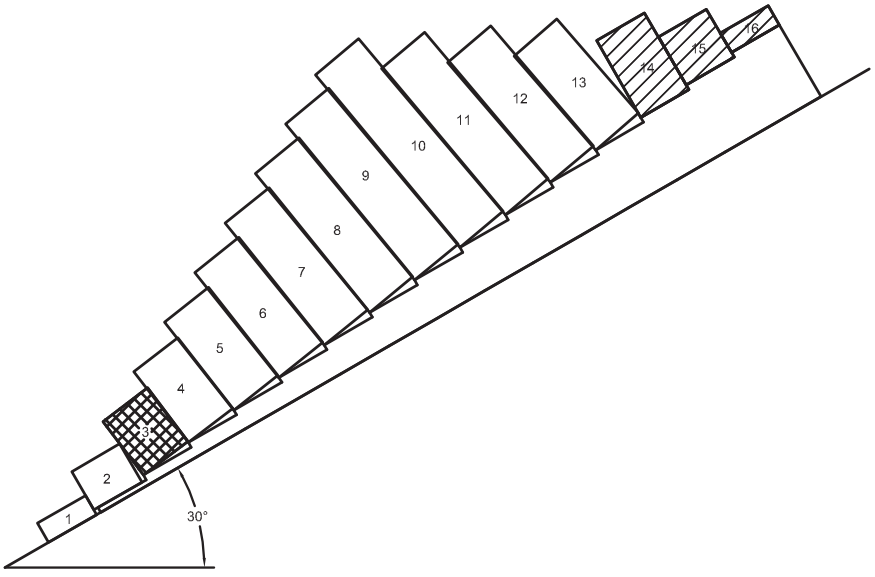

Fig. 10. Example 1 – predicted toppling mechanism for a dip or tilt angle of 30°. The three shaded blocks remain stable (14, 15, 16), two blocks slide (1, 2) and the hatched block (3) is predicted to topple by the current procedure, but to fail by sliding in the analytical solution [7].

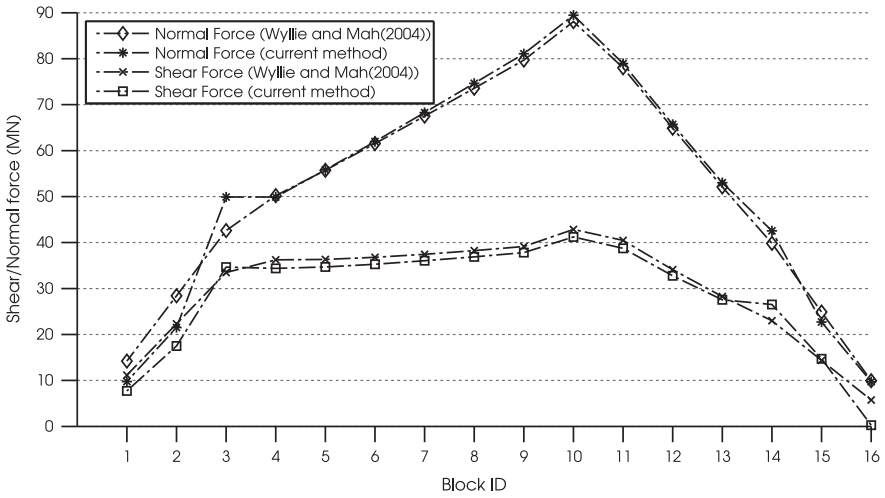

Fig. 11. Example 1 – comparison of normal and shear forces obtained using the current method and the limit equilibrium method by Goodman and Bray [7].

significant advantage of the proposed procedure is that it is much more general, and does not for example require that the supporting slope is stepped to enable the calculations to be performed.

5.2. Example 2: Ashby's staggered joints problem (experimental)

The experimental data utilised here were produced by Ashby [2]. Plaster blocks with an interface angle of friction of 36° were used to create a simplified model and were tilted to failure as shown in Fig. 12a. Initially a non-staggered pattern of blocks was used but the results were found to be variable as a consequence of shear failure across some of the columns. A staggered pattern was therefore adopted which maintained a continuous but flexible column structure and produced consistent results. In each case the tilt angle required to cause failure was determined.

The single column model failed by sliding only when the tilt angle reached the friction angle of the base (36°). As more columns were added, the tilt angle at failure reduced, as shown in Fig. 13. The particular significance of this is that if a simple sliding analysis is assumed, and the effect of toppling is ignored, the analysis will grossly overestimate the tilt angle at failure.

The same problems were modelled using the proposed non-associative method and the results compared in Fig. 13. It can be seen that the experimental results closely match the average of the min–max results, and that the initial non-associative solution and the lowest values in the min–max envelope are on the safe side. Solutions obtained assuming associative friction are also shown; these clearly grossly overestimate the tilt angle required to cause failure when more than a small number of columns of blocks are involved. Analytical results for the same problem obtained using the Goodman and Bray limit equilibrium routine are also shown. These results show that the Goodman and Bray analysis overestimates the experimental results up to 12 columns and underestimates the tilt angle for more than 12 columns, despite the assumption of continuous non-flexing columns used in this case. For the larger number of columns the Goodman and Bray analysis agrees quite well with the proposed non-associative solution.

It is also evident that the predicted failure mechanism shown in Fig. 12 has a similar form to that observed experimentally. Characteristic features for this set up include sliding of toe blocks and the presence of a triangular pocket of stable blocks at the base of the taller columns, features which were observed both experimentally and numerically. However, it is notable that whereas in the experiments the uppermost blocks were observed to slide relative to underlying toppling columns, this was not observed numerically. It is reasonable to infer that the experimentally observed mechanism is slightly less critical (i.e. involves slightly more energy dissipation) than that identified in the numerical analysis, but occurs in practice due to minor imperfections in the physical model. Another possible explanation is that whereas in the numerical model scaled up instantaneous displacements are shown, actual displacements are shown in the case of the physical model.

In summary, the proposed non-associative procedure provides reasonably good, if somewhat conservative, predictions of stability in the case of Ashby's staggered joints problem, and the min–max procedure described in Section 4 successfully brackets all the experimental results.

5.3. Example 3: Non-staggered joints problem (experimental)

Lanaro et al. [6] used physical and numerical models to simulate toppling failure of the arrangement of blocks shown in Fig. 14. The block geometry was 90 mm × 90 mm × 40 mm, with a unit weight of 28 kN/m^3 and friction angle of 38°. A total of 97 blocks were stacked into columns to form a slope.

The physical model was placed on a table which was tilted until collapse. Lanaro et al. [6] modelled the same arrangement numerically using the distinct element code UDEC [30]. Their numerical model was found to overestimate stability, with failure predicted to occur at a tilt angle of 11° in the numerical model compared with 9° experimentally. A good match was obtained when a reduced angle of friction of 31° was used in the UDEC model. Lanaro et al. [6] attribute this to possible damage of the block interfaces and to the development of large displacements at lower tilt angles in the experiments, leading to premature failure. It was suggested that this could effectively be modelled in the numerical model by using a very much lower angle of friction. To investigate this further, the same problem was analysed using the proposed numerical method. The failure mechanisms for different angles of friction are shown in Fig. 14 and the numerical results in Fig. 15.

Firstly, the predicted mechanism shown in Fig. 14a quite closely replicates the experimentally observed collapse mechanism. Secondly, from Fig. 15 it is evident that the numerical non-associative results and the min–max envelope are relatively insensitive to angle of friction. (This is in stark contrast to the associative friction results, which suggest that stability increases monotonically with increasing angle of friction.) However, at higher angles of friction ($>35°$) there is some sensitivity, and in order to obtain failure at the experimentally observed critical tilt angle of 9°, an angle of friction of 37° needs to be used. This is just 1° less than the

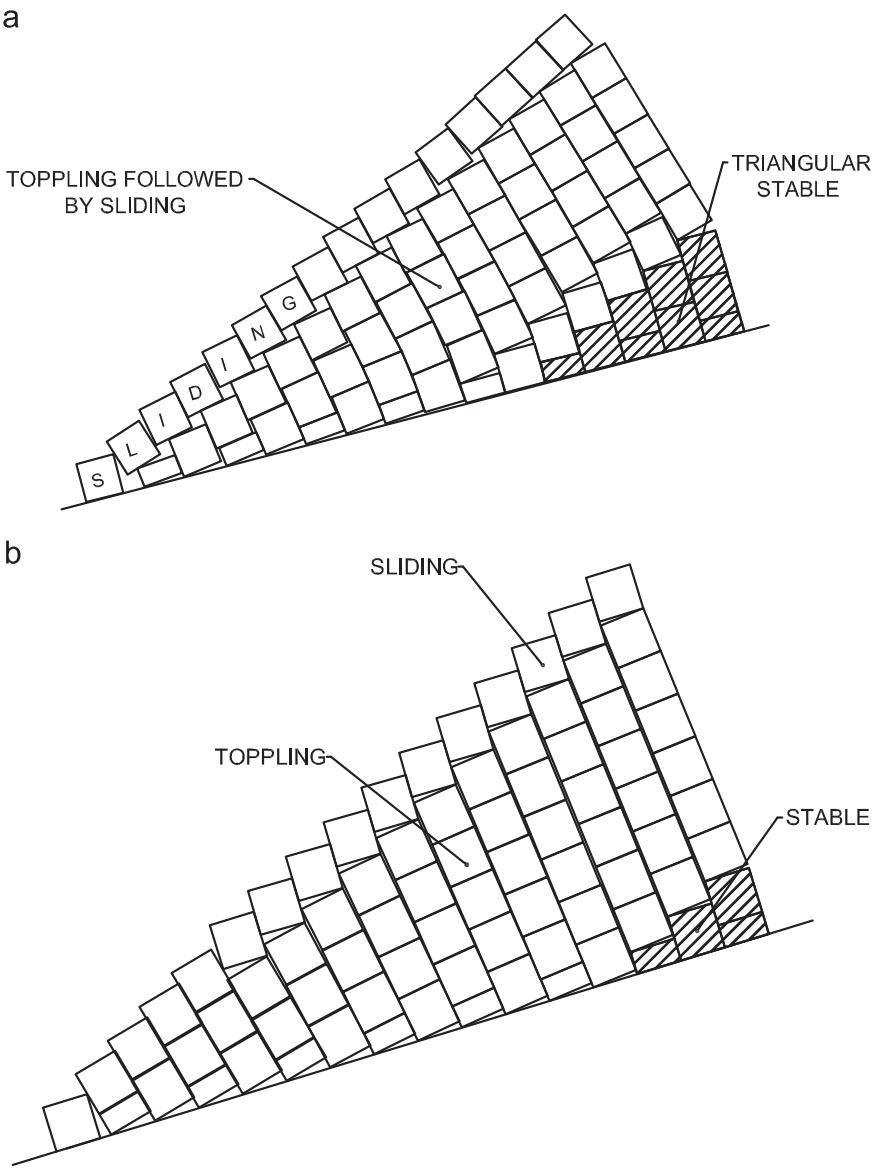

Fig. 12. Example 2 – experimental and predicted failure mechanisms, showing stable, sliding and toppling blocks. (a) Experimental results and (b) numerical results.

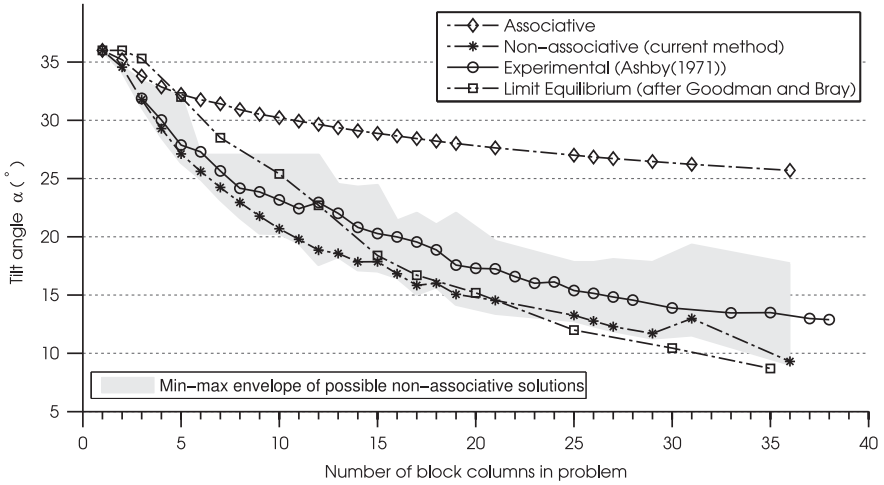

Fig. 13. Example 2 – predicted and experimental results vs. number of columns.

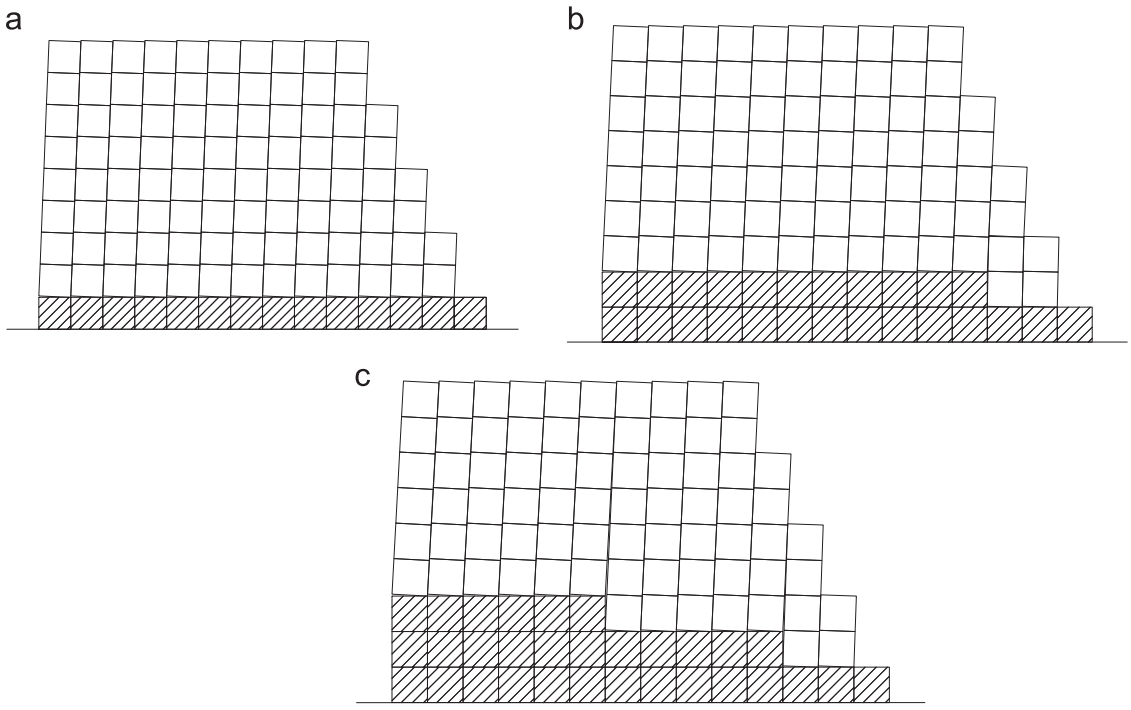

Fig. 14. Example 3 – range of predicted failure mechanisms (shaded blocks are stable). (a) $\phi=31^\circ$–35°, (b) $\phi=36^\circ$, and (c) $\phi=38^\circ$.

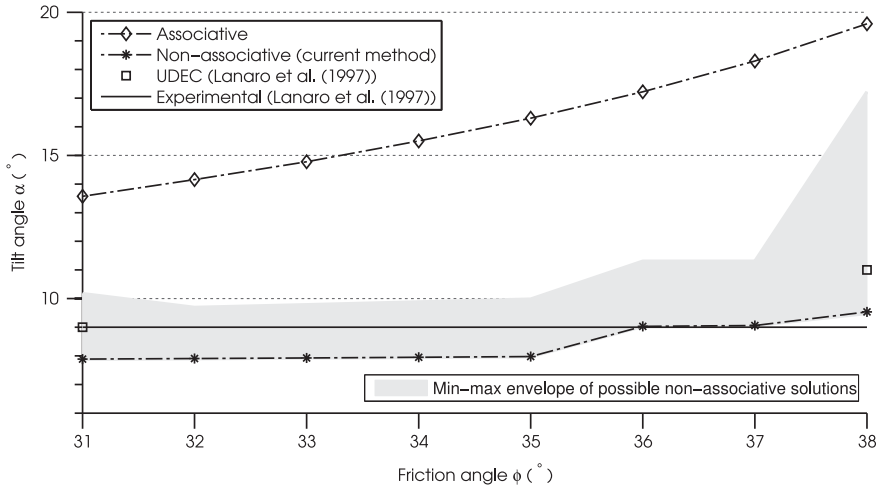

Fig. 15. Non-staggered joints problem: numerical results compared to experimental results.

measured friction, but is significantly higher than the angle of friction required in the UDEC model to replicate the experimental results (31°).

In summary, the proposed non-associative procedure provides reasonably good predictions of stability for the model studied by Lanaro et al., with the min–max procedure described in Section 4 bracketing the experimental result over a wide range of angles of friction ($31^\circ \le \phi^\circ \le 37^\circ$).

5.4. Discussion

The proposed method of generating non-associative mechanisms has been found to be capable of generating credible mechanisms very similar to those seen experimentally. However, whilst there may be several viable non-associative mechanisms, the standard procedure will only converge on one solution (assuming that this can be obtained; note that several solutions are missing from Fig. 13 because the prescribed convergence tolerance could in some cases not be met). While the converged solution is not guaranteed to be the least stable mechanism, the results obtained so far indicate that the mechanism found is generally as, or more, critical than that observed in the corresponding physical model. This is not necessarily surprising as it is likely that the physical models will have minor discrepancies from the idealised numerical model geometry, that influence the nature of the mechanism that actually forms.

Finally, although in the interests of space associative friction mechanisms have not been shown in the paper, these were generally observed to be highly unrealistic. Even more importantly, the associative friction model has been found to be prone to grossly over-predicting the critical tilt angles in the case of the experimental examples considered (e.g. 25.7° cf. a non-associative prediction of 9.3° in the case of the Ashby staggered block example involving 36 columns).

6. Conclusions

1. A numerical analysis procedure originally developed to assess the stability of masonry walls has been shown to be capable of generating kinematically viable non-associative solutions for rock toppling problems, similar or identical to those observed experimentally, or obtained using conventional limit-equilibrium techniques in the case of simple problems.
2. A significant advantage of the proposed limit analysis procedure compared with the limit equilibrium techniques that have been traditionally applied to rock toppling problems is that it is generally applicable, and does not require assumptions to be made about how forces act within the system.
3. The numerical analysis procedure has been found to provide reasonable, albeit somewhat conservative (i.e. safe), estimates of the stability of experimental rock toppling setups considered in the literature.
4. A new min–max procedure that can provide minimum and maximum non-associative solutions for a particular kinematic collapse mechanism has been described. When used in combination with the proposed non-associative numerical analysis procedure this generates solutions that successfully bracket experimental data described in the literature.
5. Conventional associative friction limit analysis models are likely to grossly over-predict the stability of rock slopes when toppling of blocks is involved, and their use should therefore be avoided.

Acknowledgments

The first author was supported by an EPSRC DTA studentship. The support of EPSRC funding under grant reference EP/I014489/1 is also gratefully acknowledged.

References

[1] Hoek E, Bray JW. Rock slope engineering. 2nd ed. . London: The Institution of Mining and Metallurgy; 1977.
[2] Ashby J. Sliding and toppling modes of failure in models and jointed rock slopes [M.Sc. thesis]. Department of Mining, Imperial College of Science & Technology, London, UK; 1971.
[3] De Freitas MH, Waters RJ. Some field examples of toppling failure. Geotechnique 1973;23(4):495–514.
[4] Cundall PA. A computer model for simulating progressive large scale movements in blocky rock systems. In: Proceedings of the symposium of International Society of Rock Mechanics. vol. 1. Nancy, France; 1971, p. 129–70.
[5] Ishida T, Chigira M, Hibino S. Application of the distinct element method for analysis of toppling observed on a fissured rock slope. Rock Mech Rock Eng 1987;20:277–83.
[6] Lanaro F, Jing L, Stephansson O, Barla G. D.E.M. modelling of laboratory tests of block toppling. Int J Rock Mech Min. Sci 1997;34(3–4):173.e1–15.
[7] Goodman RE, Bray JW. Toppling of rock slopes. In: ASCE speciality conference on rock engineering for foundations and slopes, Boulder, Colorado; vol. 2. ASCE; 1976. p. 201–34.
[8] Wyllie DC. Toppling rock slope failures examples of analysis and stabilization. Rock Mech Rock Eng 1980;13:89–98.
[9] Zanbak C. Design charts for rock slopes susceptible to toppling. J Geotech Eng ASCE 1983;109(8):1039–62.
[10] Aydan O, Kawamoto T. The stability of slopes and underground openings against flexural toppling and their stabilisation. Rock Mech Rock Eng 1992;25(3):143–65.
[11] Adhikary DP, Dyskin AV, Jewell RJ, Stewart DP. A study of the mechanism of flexural toppling failure of rock slopes. Rock Mech Rock Eng 1997;30(2):75–93.
[12] Sagaseta C, Sánchez JM, Cañizal J. A general analytical solution for the required anchor force in rock slopes with toppling failure. Int J Rock Mech Min Sci 2001;38(3):421–35.
[13] Liu CH, Jaksa MB, Meyers AG. A transfer coefficient method for rock slope toppling. Can Geotech J 2009;46(1):1–9.
[14] Tatone BSA, Grasselli G. Rocktopple: a spreadsheet-based program for probabilistic block-toppling analysis. Comput Geosci 2010;36(1):98–114.
[15] Liu CH, Jaksa MB, Meyers AG. Toppling mechanisms of rock slopes considering stabilization from the underlying rock mass. Int J Rock Mech Min Sci 2010;47(2):348–54.
[16] Amini M, Majdi A, Aydan O. Stability analysis and the stabilisation of flexural toppling failure. Rock Mech Rock Eng 2009;42(5):751–82.
[17] Alzoubi AK, Martin CD, Cruden DM. Influence of tensile strength on toppling failure in centrifuge tests. Int J Rock Mech Min Sci 2010;47(6):974–82.
[18] Majdi A, Amini M. Analysis of geo-structural defects in flexural toppling failure. Int J Rock Mech Min Sci 2011;48(2):175–86.
[19] Amini M, Majdi A, Veshadi M. Stability analysis of rock slopes against block-flexure toppling failure. Rock Mech Rock Eng 2012;45(4):519–32.
[20] Chen WF. Limit analysis and soil plasticity. Developments in geotechnical engineering. Amsterdam: Elsevier; 1975 vol. 7.
[21] Drucker DC. Coulomb friction, plasticity, and limit loads. J Appl Mech ASME 1954;21(1):71–4.
[22] Gilbert M, Casapulla C, Ahmed HM. Limit analysis of masonry block structures with non-associative frictional joints using linear programming. Comput Struct 2006;84(3):873–87.
[23] Livesley RK. Limit analysis of structures formed from rigid blocks. Int J Numer Methods Eng 1978;12(12):1853–71.
[24] Gilbert M, Melbourne C. Rigid-block analysis of masonry structures. Struct Eng 1994;72:356–61.
[25] Ferris MC, Tin-Loi F. Limit analysis of frictional block assemblies as a mathematical program with complementarity constraints. Int J Mech Sci 2001;43:209–24.
[26] Orduña A, Lourenco PB. Cap model for limit analysis and strengthening of Masonry structures. ASCE J Struct Eng 2003;129:1367–75.
[27] Mosek, The MOSEK optimization tools manual. Mosek ApS; version 5.0 ed.; 2010. URL ⟨http://www.mosek.com⟩.
[28] Charnes A, Lemke CE, Zienkiewicz OC. Virtual work, linear programming and plastic limit analysis. Proc R Soc Lond Ser A Math Phys Sci 1959;251(264):110–6.
[29] Wyllie DC, Mah CW. Rock slope engineering: civil and mining. 4th ed. London: UK Spon Press; 2004.
[30] Cundall PA. UDEC—a generalized distinct element program for modeling jointed rock. In: U.S. Army, European Research Office, London. Peter Cundall Associates; 1980, Report PCAR-1-80, Contract DAJA37-79-C-0548.